

A Robust \mathcal{H}_∞ Full-State Observer for Under-Tendon-Driven Prosthetic Hands

Julio Fajardo^{1,2}, Diego Cardona¹, Guillermo Maldonado¹, Antonio Ribas Neto^{2,3} and Eric Rohmer²

Abstract—Controlling different characteristics like force, speed and position is a relevant aspect in assistive robotics, because their interaction with diverse, common, everyday objects is divergent. Usual approaches to solve this issue involve the implementation of sensors; however, the unnecessary use of such devices increases the prosthetics' prices in a significant manner. Thus, this work focuses on the design of an \mathcal{H}_∞ full-state observer to estimate the angular position and velocity of the motor's gearhead in order to determine parameters such as the joints' torque, fingertip force and the generalized coordinates of the digits of an under-tendon-driven system to replace the transducers. This is achieved by measuring the current demanded by the brushed DC motors operating the fingers of an open-source, 3D-printed and intrinsic prosthetic hand. Besides, the proposed method guarantees disturbance attenuation, as well as the asymptotic stability of the error estimation. In addition to that, the theoretical model was validated through its implementation on a prosthetic finger, showing successful results.

Index Terms— \mathcal{H}_∞ filtering, linear matrix inequalities, full-state observer, sensor-less estimation, upper-limb prosthesis.

I. INTRODUCTION

The affordability and availability of basic prosthetic care are still limited in some parts of the world, particularly in developing countries, since their limb-impaired inhabitants cannot finance assistive technology worth \$1000 or more and, because their acquisition is not always guaranteed [1]–[4]. That is why the most common prosthetics in such places are steel hooks, which have several limitations that make them a non-competitive alternative to the more expensive and practical bionic devices. This superiority lies in their correct functioning in tandem with additional, diverse aspects looking to ameliorate the user experience, like providing feedback on their environment or the functionality of the device, even if it elevates its price. [5] Thus, aiming for a low-budget, anthropomorphic and highly functional prosthesis is relevant to provide a solution to the accomplishing of activities of daily living (ADLs), whilst incorporating additional, useful features to improve the user experience.

On the other hand, the use of sensory feedback provides the patients a more realistic substitute for their biological counterpart, conveying information as thermal, pressure, strain or vibrational stimuli [6,7]. This tactile feedback has been shown to be important, since the coordination, manipulation and grip selection whilst interacting with everyday items has been demonstrated to worsen when having a lower sensitivity [8]–[10]. However, haptics alone does not improve the user's interaction with common objects. This leads to employ different kinds of transducers to close the feedback control loops of the assistive devices to increase their usability during ADLs. For instance, the utilization of potentiometers and quadrature encoders, as well as the use of force or tactile/pressure sensors, has been used to better the functionality and the grip on items held by a prosthetic hand by controlling the speed and the strength exerted by each finger [11]–[14]. These approaches increase the price and, in some cases, the size of the prosthetics themselves, leading the patients to settle with lightweight aesthetic prostheses or to not use any at all [15,16].

To mitigate these issues, most typical solutions rely on the use of sensor-less observers, which estimate the full state of the system depending on the current or voltage measurements. These methods not only reduce the cost, weight and size of the prosthesis itself, but also offer other advantages, such as easy maintenance and reparability, since the system is considerably simplified [17]. Sensor-less observers are typically divided into two groups; the first one estimates the angular speed of the shaft based on the ripple component of the measured signal, which results from the electromotive force induced in each coil or, when the brushes in the commutator short adjacent segments [18,19]; the second is built upon the dynamic linear model of brushed DC motors and is able to estimate its own states [20]–[22].

Other approaches include the use of the brushed DC motors' non-linear model [23,24], as well as the utilization of neural networks to obtain an approximation for the resulting non-linear system, leading to more complex systems with high computational costs [25,26]. Furthermore, alternate versions consider the implementation of more specialized methods in order to improve the estimation of the states under a stochastic dynamical system. In this manner, methods such as the Kalman (KF), extended Kalman (EKF) and the particle (PF) filters provide robustness to exogenous disturbances surging from both, the process and the sensor [27]–[29].

¹ Author is with Turing Research Laboratory, FISICC, Galileo University, Guatemala City, Guatemala. {juandiego.cardona, guiller}@galileo.edu

² Author is with the Department of Computer Engineering and Industrial Automation, FEEC, UNICAMP, 13083-852 Campinas, SP, Brazil. {julioef, eric}@dca.fee.unicamp.br

³ Author is with Federal Institute of Education, Science and Technology Catarinense, 89609-000 Luzerna, SC, Brazil. antonio.ribas@ifc.edu.br

However, these errors need to be modeled as Gaussian noise, which causes issues in real applications, especially due to the manual noise covariance tuning parameters. Similarly, \mathcal{H}_∞ -based observers can also handle with such uncertainty, but only require to be energy-bounded, thus no assumptions regarding the noise are needed. In addition to that, this methodology ensures that the energy gain from the noise inputs to the estimation error ratio is limited by an upper-bound limit, which guarantees the convergence of its solution.

This work proposes a method to obtain the \mathcal{H}_∞ observer gain matrix through the use of linear matrix inequalities (LMIs) methodologies [30] in order to estimate the full state of the discrete-time model of a brushed DC motor actuating the fingers of an assistive device for transradial amputees, in this case, the Galileo Hand, an intrinsic, under-tendon-driven (UTD), upper-limb prosthesis [31,32]. In addition to that, the position and velocity of the fingers can also be estimated by measuring the current demanded by the actuators operating each finger on the artificial hand.

The notation used throughout this work is as follows: capital and lower-case bold letters stand for matrices and vectors, respectively; the rest denote scalars. For symmetric matrices, $\mathbf{P} > 0$ indicates that \mathbf{P} is positive definite; similarly with $\mathbf{P} \geq 0$ denoting it as non-negative definite. For a transfer function, $H(z)$ analytic for $|z| \geq 0$, $\|H(z)\|_2$ and $\|H(z)\|_\infty$ denote the standard \mathcal{H}_2 and \mathcal{H}_∞ norms, correspondingly. Furthermore, for the sake of easing the notation of partitioned symmetric matrices, the symbol $*$ indicates, generically, each of its symmetric blocks.

The rest of this paper is structured as follows: Section II elaborates on the UTD system used in the upper-limb prosthesis and its implications, Section III states the issues of designing an observer for the prosthetic hand described in the previous section, whilst Section IV proposes a discrete-time \mathcal{H}_∞ observer to handle with unknown measurements and process noises, as well as a method to find its gain through the utilization of LMI methods. Finally, experimental results and conclusions are presented in Sections V and VI, accordingly.

II. THE UNDER-TENDON-DRIVEN MACHINE

The Galileo Hand is an affordable, open-source, anthropomorphic and UTD myoelectric upper-limb prosthesis for transradial amputees, whose intrinsic design allows for individual finger control [31,32]. These digits are conformed by three phalanges: distal, proximal and middle; as well as three joints: distal and proximal interphalangeal (DIP and PIP) and the metacarpophalangeal (MCP) one (illustrated in Fig. 1). Thus, each finger possesses 3 degrees of freedom (DOF); but, since each one is operated by a single motor, only one degree of actuation (DOA). Such a system permits the extension and flexion of each member by operating its two tendons; an active and a passive one, which run along the internal canals inside the finger (the blue sections in Fig. 1). The first one consists of a waxed nylon cord extended along the finger's

dorsal side, which is actuated by a brushed DC motor with a gear ratio of 250:1; thus, generating a positive tensile force, f_{ta} , that flexes the finger. The second one is composed by a round, surgical-grade elastic going through the duct inside the digit's volar face; this results in a passive tensile force, f_{te} , opposing itself to the actuator's drive that depends uniquely on the joints' deflection, resulting in springing the limb back open [33].

Thus, letting L be the number of tendons; N the amount of joints; and $\mathbf{f}_t \in \mathbb{R}^L \ni \mathbf{f}_t = [f_{ta} \ f_{te}]^T$, the tensile force vector, a relationship between the joint torque vector, $\boldsymbol{\tau} \in \mathbb{R}^N$, can be given by

$$\boldsymbol{\tau} = -\mathbf{J}_j^T \mathbf{f}_t \quad (1)$$

where $\mathbf{J}_j = [\mathbf{J}_{ja} \ \mathbf{J}_{je}]^T$ is the Jacobian matrix for the active and passive tendons.

Furthermore, considering r is the radius of the joint's pulleys and, taking into account the tendon-driven machine described before (resulting in $L = 2$ and $N = 3$), the following is true for each finger

$$\mathbf{J}_j = \begin{bmatrix} r & r & r \\ -r & -r & -r \end{bmatrix} \quad (2)$$

Alternatively, the tensile force vector for the system can also be defined by the following equation.

$$\mathbf{f}_t = \mathbf{f}_b - (\mathbf{J}_j^T)^+ \boldsymbol{\tau} \quad (3)$$

where $(\mathbf{J}_j^T)^+$ is the Moore-Penrose pseudoinverse of the transposed Jacobian matrix, and $\mathbf{f}_b \in \mathbb{R}^L$ is a bias force vector that prevents the tendons from loosening and does not have an impact on $\boldsymbol{\tau}$, which is defined as follows

$$\mathbf{f}_b = \mathbf{A}\boldsymbol{\xi}, \quad \mathbf{A} = [\mathbf{I}_L - (\mathbf{J}_j^T)^+ \mathbf{J}_j^T] \quad (4)$$

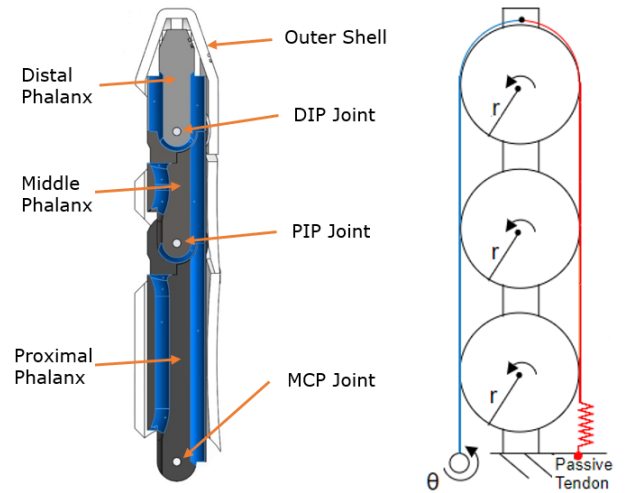


Fig. 1: Mechanical design for the fingers, where r is the pulley's radius; and θ , the gearhead shaft's angular position.

such that ξ is a compatible dimensional vector with \mathbf{A} and \mathbf{I}_L is the identity matrix of size L .

Considering the previous equations, the relationship between the generalized coordinates, \mathbf{q} , and the motor angle vector, θ , can be defined as the following

$$\mathbf{q} = \mathbf{J}_j^+ [\mathbf{l} - \mathbf{l}_0 - \mathbf{J}_a \theta] + \mathbf{q}_0 \quad (5)$$

where $\mathbf{l} = [l_a \ l_e]^T$ is the deflection of the tendons, such that l_a and l_e are the expansion of active and passive ones, respectively; $\mathbf{l}_0 = [0 \ l_{e0}]^T$, an initial expansion of the tendons to prevent them from loosening; \mathbf{q}_0 , an initial angular displacement of the joints; and \mathbf{J}_a , the Jacobian matrix related to the actuator.

Therefore, since a positive initial expansion of the passive tendon l_{e0} is considered for each finger, it is evident that the bias force $f_b > 0$, resulting in a tendon-driven machine and, moreover, since $\text{rank}(\mathbf{J}_j) = 1 < \mathbf{N}$, the system is, additionally, a UTD mechanism.

Furthermore, the dynamic equations of the tendon-driven system are given by the following equations

$$\mathbf{M}\ddot{\mathbf{q}} + \left[\frac{1}{2}\dot{\mathbf{M}} + \mathbf{S} + \mathbf{B}_0 \right] \dot{\mathbf{q}} + \mathbf{G}_g \mathbf{q} = \boldsymbol{\tau} \quad (6)$$

$$J_m \ddot{\theta} + b \dot{\theta} + r_p f_{ta} = \tau_m \quad (7)$$

where \mathbf{M} and \mathbf{B}_0 are the inertia and damping matrices of the finger, accordingly, \mathbf{S} is a skew-symmetric matrix and \mathbf{G}_g is the gravity load matrix. Additionally, J_m and b are the gearhead's moment of inertia and friction coefficient, correspondingly; τ_m , the torque exerted by the motor gearhead's shaft; and r_p , the radius of the pulley mounted on it [33].

III. PROBLEM STATEMENT

Since the dynamic behavior of the finger is non-linear, particularly due to the inertia matrix and the centripetal and Coriolis terms expressed in Eq. (6), one cannot simply estimate the full state of the coupled system of differential equations, (6)-(7). Thus, an approximated linear model was created instead, which considers the dynamic equations of the finger as a mass-spring system, whose behavior is similar to that of a UTD machine (as the passive tendon opposes itself to the flexion movement, but favors the extension one). In addition, this also simplifies the computational load, since it is not necessary to linearize the model on each operating point, permitting its implementation on the microcontroller unit (MCU) used on the prosthetic device.

Furthermore, the mechanism that drives the fingers does not have a mechanical limit to cease the extension movement, causing the motor to continue actuating the digit and flexing it again (as the pulley coils the string in the opposite direction). Therefore, the purpose of implementing such an observer is to determine the state of the fingers (opened or closed) using the estimation of the angular displacement of the gearhead's shaft only, leading to not requiring an exact result for the

generalized coordinates \mathbf{q} . However, an approximation for it can still be determined from Eq. (5); similarly with the joints' torque, $\boldsymbol{\tau}$ from Eq. (6).

Considering G_r as the gear ratio, k_t as the motor's constant, i_a as the current it demands, and η as the gearhead's efficiency, τ_m can be obtained with the following expression:

$$\tau_m = \eta G_r k_t i_a \quad (8)$$

In this way, the continuous-time model for a brushed DC motor in the space state results in:

$$\dot{\mathbf{x}} = \begin{bmatrix} 0 & 1 & 0 \\ -\frac{k_e r_p^2}{J_m} & -\frac{b}{J_m} & \frac{\eta G_r k_t}{J_m} \\ 0 & -\frac{k_t}{L_a} & -\frac{R_a}{L_a} \end{bmatrix} \mathbf{x} + \begin{bmatrix} 0 \\ 0 \\ \frac{1}{L_a} \end{bmatrix} u \quad (9)$$

$$\mathbf{y} = [0 \ 0 \ 1] \mathbf{x} \quad (10)$$

where $\mathbf{x} = [\theta \ \dot{\theta} \ i_a]^T$, with θ and $\dot{\theta}$ being the gearhead's angular position and velocity, respectively; k_e is the elastic constant of the passive tendon; L_a is the motor's inductance; R_a and u are the armature's resistance and voltage, accordingly; and y is the measured output.

IV. DISCRETE-TIME \mathcal{H}_∞ FULL-STATE OBSERVER

For designing the observer, a discretization of the aforementioned system is required. Considering the noise components and a sampling time k , it results in the following:

$$\mathbf{x}_{k+1} = \mathbf{A}\mathbf{x}_k + \mathbf{B}_1 \mathbf{u}_k + \mathbf{B}_2 \mathbf{w}_k \quad (11)$$

$$\mathbf{y}_k = \mathbf{C}\mathbf{x}_k + \mathbf{D}_1 \mathbf{v}_k + \mathbf{D}_2 \mathbf{w}_k \quad (12)$$

where $\mathbf{x}_k \in \mathbb{R}^n$, $\mathbf{u}_k \in \mathbb{R}^p$, $\mathbf{y}_k \in \mathbb{R}^q$, $\mathbf{w}_k \in \mathbb{R}^s$ and $\mathbf{v}_k \in \mathbb{R}^t$ are the states, control input, measured output, process and measurement noise vectors, respectively. Besides, $\mathbf{A} \in \mathbb{R}^{n \times n}$, $\mathbf{B}_1 \in \mathbb{R}^{n \times p}$, $\mathbf{B}_2 \in \mathbb{R}^{n \times s}$, $\mathbf{C} \in \mathbb{R}^{q \times n}$, $\mathbf{D}_1 \in \mathbb{R}^{q \times t}$ and $\mathbf{D}_2 \in \mathbb{R}^{q \times s}$ are the process, input control and input process noise, measured output, as well as the output process and output sensor noise matrices, correspondingly. Then, by defining a general noise vector, $\tilde{\mathbf{w}}_k = [\mathbf{w}_k \ \mathbf{v}_k]^T$, an observer-based filter can be described by

$$\hat{\mathbf{x}}_{k+1} = \mathbf{A}\hat{\mathbf{x}}_k + \mathbf{B}_1 \mathbf{u}_k - \mathbf{K}(\mathbf{y}_k - \hat{\mathbf{y}}_k) \quad (13)$$

where $\hat{\mathbf{x}}_k \in \mathbb{R}^n$ is the estimated state; $\hat{\mathbf{y}}_k \in \mathbb{R}^n$ the estimated output; and \mathbf{K} , the observer gain.

Since the initial conditions of the estimated state, $\hat{\mathbf{x}}_0$, are equal to those of the initial state, $\mathbf{x}_0 = [0 \ 0 \ 0]^T$, one can determine the filtering error dynamic, from the expressions (11)-(13), with the following augmented system:

$$\mathbf{e}_{k+1} = \tilde{\mathbf{A}}\mathbf{e}_k + \tilde{\mathbf{B}}\tilde{\mathbf{w}}_k \quad (14)$$

$$\tilde{\mathbf{y}}_k = \tilde{\mathbf{C}}\mathbf{e}_k + \tilde{\mathbf{D}}\tilde{\mathbf{w}}_k \quad (15)$$

with

$$\begin{aligned}\tilde{\mathbf{A}} &= \mathbf{A} + \mathbf{K}\mathbf{C}, & \tilde{\mathbf{B}} &= [\mathbf{B}_2 + \mathbf{K}\mathbf{D}_2 \quad \mathbf{K}\mathbf{D}_1] \\ \tilde{\mathbf{C}} &= \mathbf{C}, & \tilde{\mathbf{D}} &= [\mathbf{D}_2 \quad \mathbf{D}_1]\end{aligned}$$

The main goal is to find an optimal robust observer-based filter for the system composed by (11) and (12), where the error filtering, \mathbf{e}_k , has to satisfy that $\|\mathbf{e}_k\|_2 \leq \gamma(\|\mathbf{w}_k\|_2 + \|\mathbf{v}_k\|_2)$, with the robustness level $\gamma \in \mathbb{R} \ni \gamma > 0$. Therefore, from the bounded-real lemma and given the transfer function $H(z)$ in the complex frequency-domain for the system (14-15), the norm \mathcal{H}_∞ can be characterized using the Lyapunov function, $\nu(\mathbf{x}_k) = \mathbf{x}_k^T \mathbf{P} \mathbf{x}_k$, as done in [34], imposing that

$$\|H(z)\|_\infty < \gamma \Leftrightarrow \exists \mathbf{P} \in \mathbb{R}^{n \times n} \ni \mathbf{P} = \mathbf{P}^T \geq 0 \quad (16)$$

Hence, an observer meeting the aforementioned requirements can be successfully established if a solution to the following convex optimization problem can be found

$$\min_{\mathbf{Z}, \mathbf{P}=\mathbf{P}^T > 0} \gamma \quad (17)$$

which is subject to the following LMI

$$\begin{bmatrix} \mathbf{P} & \mathbf{A}^T \mathbf{P} + \mathbf{C}^T \mathbf{Z}^T & \mathbf{0}_{n \times s} & \mathbf{0}_{n \times s} & \mathbf{C}^T \\ * & \mathbf{P} & \mathbf{P}\mathbf{B}_2 + \mathbf{Z}\mathbf{D}_2 & \mathbf{Z}\mathbf{D}_1 & \mathbf{0}_{n \times q} \\ * & * & \mathbf{I}_s & \mathbf{0}_{s \times s} & \mathbf{D}_2^T \\ * & * & * & \mathbf{I}_s & \mathbf{D}_1^T \\ * & * & * & * & \gamma^2 \mathbf{I}_q \end{bmatrix} > \mathbf{0} \quad (18)$$

where the matrices $\mathbf{Z} \in \mathbb{R}^{n \times q}$ and \mathbf{P} are the variables of the problem [30]. In addition to that, $\mathbf{K} \in \mathbb{R}^{n \times q}$ can be recovered using the following expression

$$\mathbf{K} = \mathbf{P}^{-1} \mathbf{Z} \quad (19)$$

On the other hand, to further improve this system's robustness, a slack variable, $\mathbf{G} \in \mathbb{R}^{n \times n}$, can be incorporated so that the optimization problem is now

$$\min_{\mathbf{Z}, \mathbf{G}, \mathbf{P}=\mathbf{P}^T > 0} \gamma \quad (20)$$

subjected to the following LMI

$$\begin{bmatrix} \mathbf{P} & \mathbf{A}^T \mathbf{G} + \mathbf{C}^T \mathbf{Z}^T & \mathbf{0}_{n \times s} & \mathbf{0}_{n \times s} & \mathbf{C}^T \\ * & \mathbf{G} + \mathbf{G}^T - \mathbf{P} & \mathbf{G}^T \mathbf{B}_2 + \mathbf{Z}\mathbf{D}_2 & \mathbf{Z}\mathbf{D}_1 & \mathbf{0}_{n \times q} \\ * & * & \mathbf{I}_s & \mathbf{0}_{s \times s} & \mathbf{D}_2^T \\ * & * & * & \mathbf{I}_s & \mathbf{D}_1^T \\ * & * & * & * & \gamma^2 \mathbf{I}_q \end{bmatrix} > \mathbf{0} \quad (21)$$

Moreover, since $\mathbf{G} + \mathbf{G}^T > \mathbf{P} > 0$, this implies that \mathbf{G} is non-singular [30], resulting in \mathbf{K} being able to be recovered by evaluating the equation mentioned underneath.

$$\mathbf{K} = (\mathbf{G}^T)^{-1} \mathbf{Z} \quad (22)$$

V. RESULTS

The experiments to test and validate the methods proposed in Sections III and IV were carried out using the index finger of the Galileo Hand, which is controlled by a customized board located on the inside of the palm of the artificial hand, with its volar side in a supine position [31,32]. Additionally, to design the robust \mathcal{H}_∞ observer-based filter and to solve the convex optimization problems subjected to the LMIs described in Eqs. (17)-(22), MATLAB, YALMIP and MOSEK were employed [35,36]. Later, with the resulting gain, the observer described in Eq. (13) was implemented on the MCU (ARM Cortex-M4 architecture) actuating the fingers of the assistive device.

In this way, a current on-off controller was used to determine when the finger is closed or grabbing some object, whereas, based on the encoder measurements (the ground truth), a PID position controller was implemented to fully open the finger. This leads to what is shown in Fig. 2, which illustrates the flexion and extension processes of the finger. On the upper graph, the estimation of the angular displacement, $\hat{\theta}$, is juxtaposed to its ground truth alternative, θ , whilst the lower one represents the current measured on the Shunt resistor installed on the motor driver. The aforementioned estimation was established based on the data gathered by a 100 Hz reading of a quadrature encoder and the on-chip ADC, respectively. Furthermore, the angular displacement of the motor gearhead's shaft when the finger is completely flexed, is about 4.5971 rad; while its estimated value, of 4.6775 rad. This implies that the active tendon was coiled around 16.5 mm, as opposed to the 16.8 mm estimation. A similar discrepancy occurs on the extension process, where that error is, approximately, 7.2×10^{-3} mm. So, this results in a root mean square error (RMSE) for θ of about 0.1394 rad and a robustness level, γ , of 2.2915×10^{-6} .

Besides, a comparison at different points in time between the experimental and estimated results for \mathbf{q} was established (shown in Fig. 3), considering it can be calculated by Eq. (5).

Moreover, utilizing the aforementioned results for $\hat{\mathbf{q}}$, one can determine the resulting torque on each of the joints' axes using the Eq. (6). This can be visualized in Fig. 4, where the torques exerted on the MCP, PIP and DIP joints correspond to τ_1 , τ_2 and τ_3 , accordingly.

VI. CONCLUSIONS

A simplified dynamic model of the finger, together with the design of an \mathcal{H}_∞ observer-based filter (without making any assumptions regarding the effects of noise) has proven to be a successful alternative to installing sensors for the estimation of the angular position of the motor gearhead's shaft from an under-tendon-driven prosthesis for transradial amputees, as can be seen in Fig. 2. Since the purpose of an artificial hand is to determine whether the fingers are fully closed, opened or grasping an object, rather than a precise position and orientation of the fingertips, the estimation error obtained is sufficient for the apt fulfillment of ADLs.

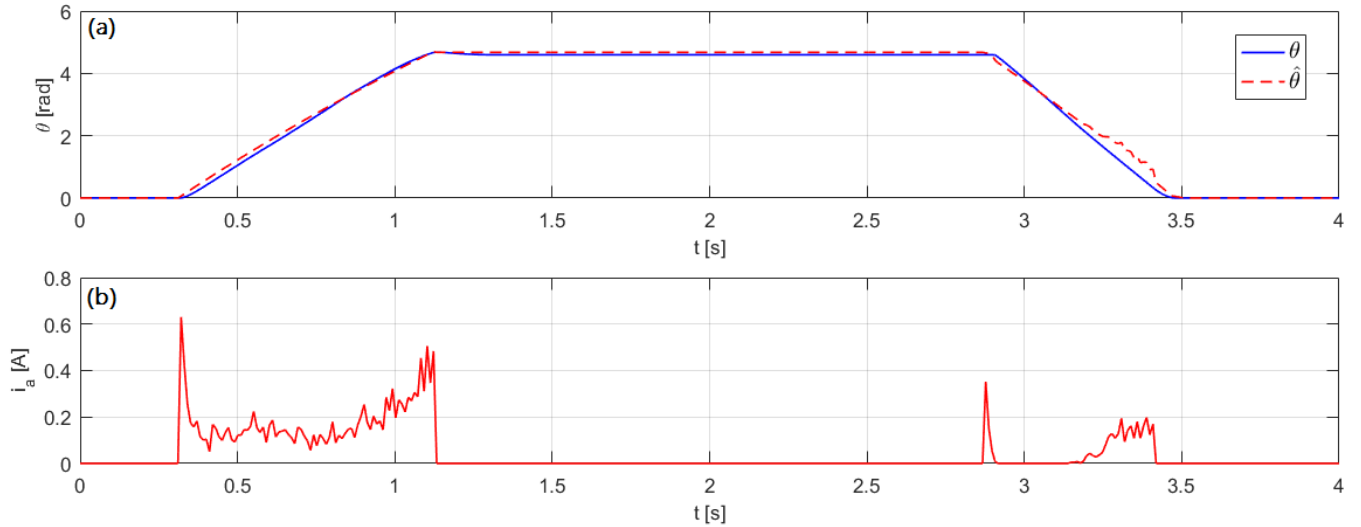


Fig. 2: (a) Motor gearhead shaft's angular displacement, θ . The dotted red line represents the estimation $\hat{\theta}$; while the solid blue line, the ground truth measured with a quadrature encoder. (b) Current measured on the motor's armature, i_a .

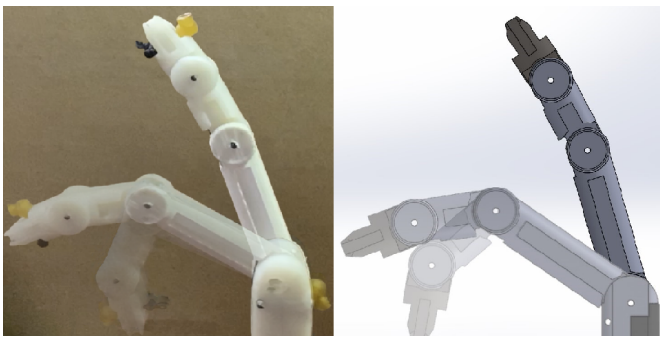


Fig. 3: Finger movement processes: the ground truth and its estimation, from left to right, respectively, where the movement starts in \mathbf{q}_0 .

Additionally, this data can be used to determine the kinematics and dynamics of each finger of the assistive device by estimating its generalized coordinates, as shown in Figs. 3 and 4, and employ this information in robust torque and impedance controllers. Moreover, such a model enables its implementation in an MCU, allowing for a more compact and affordable option to install on prosthetics.

Furthermore, observing the comportment of the torques' behaviour, shown in Fig. 4, one can trace the finger's movements as it flexes and extends. The first main peak indicates when the motor starts to coil the string, leading the motor, the elastic and the joints to have to overcome the static friction coefficient to start mobilizing; therefore a higher tensile force (and torque) has to be exerted (Fig. 5). Additionally, the second peak is a negative one, as the actuator breaks, which causes it to spin in the opposite direction; similarly, with the extension process. Other relevant aspects to note on Fig. 4 are the offsets in torque and the fact that their

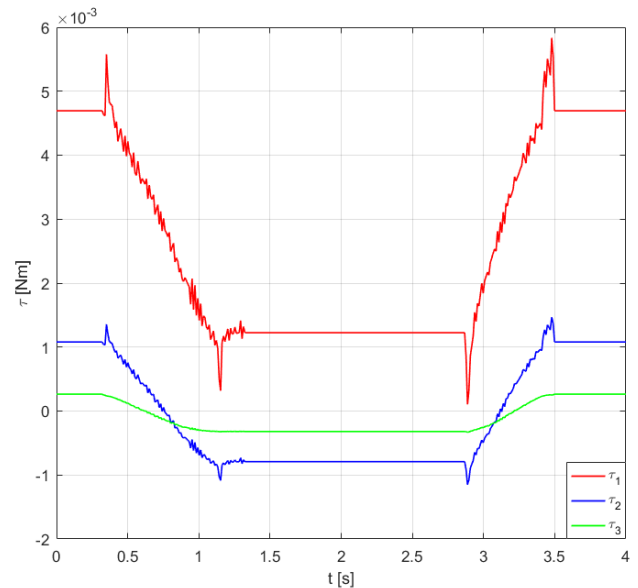


Fig. 4: Torque τ applied on the MCP, PIP and DIP joints' axes (τ_1, τ_2 and τ_3 , correspondingly).

derivatives and peaks increase in magnitude as they are closer to the metacarpus. The first one depends on the gravitational energy impacting each joint, while the latter is consequence of moving a larger lever as the joints are farther from the fingertip. In addition to that, a change in the direction of the torque is also palpable in the DIP and PIP joints, because their coordinate systems are modified as the proximal and middle phalanges rotate. Analyzing the graph permits to corroborate the functionality of the prosthesis and facilitates the pairing with a robust controller to properly regulate the prosthetic hand's overall torque to improve its grips.

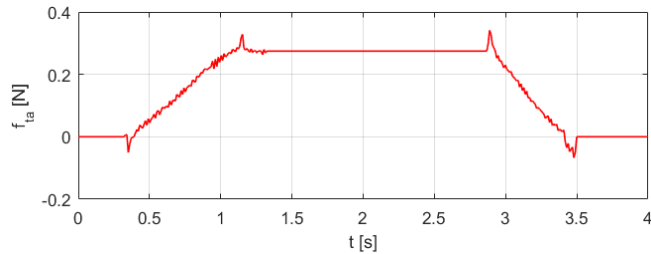


Fig. 5: Active tensile force f_{ta} exerted during the process.

Finally, despite the disturbances presented in the current measurement, as shown in Fig. 2 (3 – 3.5 s), the methods proposed in this work behaves as expected, reducing the effects of noise on estimation. This can be improved by designing a robust, full-order filter, also based on LMI methods, guaranteeing a lower robustness level. On the other hand, a better approximation of the model employing the Takagi-Sugeno technique could handle the uncertainties in a better way, both for the robust observer and the controller.

REFERENCES

- [1] D. Pilling, P. Barrett, and M. Floyd, “Disabled people and the internet: Experiences, barriers and opportunities,” 2004.
- [2] W. H. Organization *et al.*, “World report on disability: World health organization; 2011.”
- [3] D. Cummings, “Prosthetics in the developing world: a review of the literature,” *Prosthetics and orthotics international*, vol. 20, no. 1, pp. 51–60, 1996.
- [4] J. Ten Kate, G. Smit, and P. Breedveld, “3d-printed upper limb prostheses: a review,” *Disability and Rehabilitation: Assistive Technology*, vol. 12, no. 3, pp. 300–314, 2017.
- [5] C. A. Caspers, “Pressure/temperature monitoring device for prosthetics,” Dec. 19 2006, uS Patent 7,150,762.
- [6] A. Chortos, J. Liu, and Z. Bao, “Pursuing prosthetic electronic skin,” *Nature materials*, vol. 15, no. 9, p. 937, 2016.
- [7] M. C. Jimenez and J. A. Fishel, “Evaluation of force, vibration and thermal tactile feedback in prosthetic limbs,” in *2014 IEEE Haptics Symposium (HAPTICS)*. IEEE, 2014, pp. 437–441.
- [8] J. Rothwell, M. Traub, B. Day, J. Obeso, P. Thomas, and C. Marsden, “Manual motor performance in a deafferented man,” *Brain*, vol. 105, no. 3, pp. 515–542, 1982.
- [9] R. S. Johansson and G. Westling, “Roles of glabrous skin receptors and sensorimotor memory in automatic control of precision grip when lifting rougher or more slippery objects,” *Experimental brain research*, vol. 56, no. 3, pp. 550–564, 1984.
- [10] J. Monzée, Y. Lamarre, and A. M. Smith, “The effects of digital anesthesia on force control using a precision grip,” *Journal of neurophysiology*, vol. 89, no. 2, pp. 672–683, 2003.
- [11] A. Cranny, D. Cotton, P. Chappell, S. Beeby, and N. White, “Thick-film force, slip and temperature sensors for a prosthetic hand,” *Measurement Science and Technology*, vol. 16, no. 4, p. 931, 2005.
- [12] C. Cipriani, M. Controzzi, and M. C. Carozza, “The smarhand transradial prosthesis,” *Journal of neuroengineering and rehabilitation*, vol. 8, no. 1, p. 29, 2011.
- [13] A. Akhtar, K. Y. Choi, M. Fatina, J. Cornman, E. Wu, J. Sombeck, C. Yim, P. Slade, J. Lee, J. Moore *et al.*, “A low-cost, open-source, compliant hand for enabling sensorimotor control for people with transradial amputations,” in *2016 38th Annual International Conference of the IEEE Engineering in Medicine and Biology Society (EMBC)*. IEEE, 2016, pp. 4642–4645.
- [14] L. Jiang, B. Zeng, S. Fan, K. Sun, T. Zhang, and H. Liu, “A modular multisensory prosthetic hand,” in *2014 IEEE International Conference on Information and Automation (ICIA)*. IEEE, 2014, pp. 648–653.
- [15] E. National Academies of Sciences, Medicine *et al.*, *The promise of assistive technology to enhance activity and work participation*. National Academies Press, 2017.
- [16] S.-K. Sul, *Control of electric machine drive systems*. John Wiley & Sons, 2011, vol. 88.
- [17] E. Vazquez-Sanchez, J. Sottile, and J. Gomez-Gil, “A novel method for sensorless speed detection of brushed dc motors,” *Applied Sciences*, vol. 7, no. 1, p. 14, 2017.
- [18] G. C. Sincero, J. Cros, and P. Viarouge, “Arc models for simulation of brush motor commutations,” *IEEE transactions on magnetics*, vol. 44, no. 6, pp. 1518–1521, 2008.
- [19] T. Figarella and M. Jansen, “Brush wear detection by continuous wavelet transform,” *Mechanical systems and signal processing*, vol. 21, no. 3, pp. 1212–1222, 2007.
- [20] P. Chevrel and S. Siala, “Robust dc-motor speed control without any mechanical sensor,” in *Proceedings of the 1997 IEEE international conference on control applications*. IEEE, 1997, pp. 244–246.
- [21] S. Yachiangkam, C. Prapanavarat, U. Yungyuen, and S. Po-ngam, “Speed-sensorless separately excited dc motor drive with an adaptive observer,” in *2004 IEEE Region 10 Conference TENCON 2004.*, vol. 500. IEEE, 2004, pp. 163–166.
- [22] S. R. Bowes, A. Sevinc, and D. Holliday, “New natural observer applied to speed-sensorless dc servo and induction motors,” *IEEE transactions on industrial electronics*, vol. 51, no. 5, pp. 1025–1032, 2004.
- [23] C. E. Castaneda, A. G. Loukianov, E. N. Sanchez, and B. Castillo-Toledo, “Discrete-time neural sliding-mode block control for a dc motor with controlled flux,” *IEEE Transactions on Industrial Electronics*, vol. 59, no. 2, pp. 1194–1207, 2011.
- [24] Z. Z. Liu, F. L. Luo, and M. H. Rashid, “Speed nonlinear control of dc motor drive with field weakening,” *IEEE Transactions on Industry Applications*, vol. 39, no. 2, pp. 417–423, 2003.
- [25] F. Farkas, S. Halász, and I. Kádár, “Speed sensorless neuro-fuzzy controller for brush type dc machines,” in *Proceedings of the 5th International Symposium of Hungarian Researchers on Computational Intelligence, Budapest, Hungary*, 2004, pp. 11–12.
- [26] S. Weerasooriya and M. A. El-Sharkawi, “Identification and control of a dc motor using back-propagation neural networks,” *IEEE transactions on Energy Conversion*, vol. 6, no. 4, pp. 663–669, 1991.
- [27] S. Praesomboon, S. Athaphaisal, S. Yimman, R. Boontawan, and K. Dejhan, “Sensorless speed control of dc servo motor using kalman filter,” in *2009 7th International Conference on Information, Communications and Signal Processing (ICICIS)*. IEEE, 2009, pp. 1–5.
- [28] A. Khalid and A. Nawaz, “Sensor less control of dc motor using kalman filter for low cost cnc machine,” in *2014 International Conference on Robotics and Emerging Allied Technologies in Engineering (iCREATE)*. IEEE, 2014, pp. 180–185.
- [29] O. Aydogmus and M. F. Talu, “Comparison of extended-kalman-and particle-filter-based sensorless speed control,” *IEEE Transactions on Instrumentation and Measurement*, vol. 61, no. 2, pp. 402–410, 2011.
- [30] M. C. De Oliveira, J. C. Geromel, and J. Bernussou, “Extended H_2 and H_∞ norm characterizations and controller parametrizations for discrete-time systems,” *International Journal of Control*, vol. 75, no. 9, pp. 666–679, 2002.
- [31] J. Fajardo, V. Ferman, A. Lemus, and E. Rohmer, “An affordable open-source multifunctional upper-limb prosthesis with intrinsic actuation,” in *2017 IEEE Workshop on Advanced Robotics and its Social Impacts (ARSO)*. IEEE, 2017, pp. 1–6.
- [32] J. Fajardo, V. Ferman, D. Cardona, G. Maldonado, A. Lemus, and E. Rohmer, “Galileo hand: An anthropomorphic and affordable upper-limb prosthesis,” *IEEE Access*, vol. 8, pp. 81 365–81 377, 2020.
- [33] R. Ozawa, K. Hashirii, and H. Kobayashi, “Design and control of underactuated tendon-driven mechanisms,” in *2009 IEEE International Conference on Robotics and Automation*. IEEE, 2009, pp. 1522–1527.
- [34] S. Boyd, L. El Ghaoui, E. Feron, and V. Balakrishnan, *Linear matrix inequalities in system and control theory*. Siam, 1994, vol. 15.
- [35] M. ApS, “The MOSEK optimization toolbox for MATLAB,” *User’s Guide and Reference Manual, version*, vol. 4, 2019.
- [36] J. Lofberg, “YALMIP: A toolbox for modeling and optimization in MATLAB,” in *2004 IEEE international conference on robotics and automation (IEEE Cat. No. 04CH37508)*. IEEE, 2004, pp. 284–289.